Plant, Cell & Environment

Plant, Cell and Environment (2017) **40**, 378–389 doi: 10.1111/pce.12872

Original Article

Dissecting the Photoprotective Mechanism Encoded by the *flv4-2* Operon: a Distinct Contribution of Sll0218 in Photosystem II Stabilization

Luca Bersanini[1], Yagut Allahverdiyeva[1], Natalia Battchikova[1], Steffen Heinz[2], Maija Lespinasse[1], Essi Ruohisto[1], Henna Mustila[1], Jörg Nickelsen[2], Imre Vass[3] & Eva-Mari Aro[1]

[1]*Department of Biochemistry, Molecular Plant Biology, University of Turku, FI-20014 Turku, Finland,* [2]*Molecular Plant Sciences, Ludwig-Maximillians-Universität München, Biozentrum, Grosshaderner Straße 2-4, 82152 Planegg-Martinsried, Germany and* [3]*Institute of Plant Biology, Biological Research Centre of the Hungarian Academy of Sciences, P.O. Box 521, H-6701 Szeged, Hungary*

ABSTRACT

In *Synechocystis* sp. PCC 6803, the *flv4-2* operon encodes the flavodiiron proteins Flv2 and Flv4 together with a small protein, Sll0218, providing photoprotection for Photosystem II (PSII). Here, the distinct roles of Flv2/Flv4 and Sll0218 were addressed, using a number of *flv4-2* operon mutants. In the Δ*sll0218* mutant, the presence of Flv2/Flv4 rescued PSII functionality as compared with Δ*sll0218-flv2*, where neither Sll0218 nor the Flv2/Flv4 heterodimer are expressed. Nevertheless, both the Δ*sll0218* and Δ*sll0218-flv2* mutants demonstrated deficiency in accumulation of PSII proteins suggesting a role for Sll0218 in PSII stabilization, which was further supported by photoinhibition experiments. Moreover, the accumulation of PSII assembly intermediates occurred in Sll0218-lacking mutants. The YFP-tagged Sll0218 protein localized in a few spots per cell at the external side of the thylakoid membrane, and biochemical membrane fractionation revealed clear enrichment of Sll0218 in the PratA-defined membranes, where the early biogenesis steps of PSII occur. Further, the characteristic antenna uncoupling feature of the Δ*flv4-2* operon mutants is shown to be related to PSII destabilization in the absence of Sll0218. It is concluded that the Flv2/Flv4 heterodimer supports PSII functionality, while the Sll0218 protein assists PSII assembly and stabilization, including optimization of light harvesting.

Key-words: Cyanobacteria; flavodiiron proteins; photoprotection; photosynthesis; Photosystem II repair.

INTRODUCTION

The oxygenic photosynthetic machinery of cyanobacteria is sensitive to environmental changes occurring in light intensity and temperature as well as to fluctuations in availability of nutrients. In particular, the effects of inorganic carbon fluctuations have been extensively studied. When the CO_2 concentration is high (HC), the Calvin–Benson–Bassham (CBB) cycle becomes an efficient sink for the electrons produced by the water splitting activity of Photosystem II (PSII) and cyanobacteria do grow faster (MacKenzie *et al.* 2004). However, during the shift to air level CO_2 concentrations (low CO_2, LC), the photosynthetic reactions are constrained: CO_2 becomes a limiting factor, slowing down the efficiency of CBB cycle and causing an over-accumulation of electrons in photosynthetic electron transfer chain (ETC). The strong expression of carbon concentrating mechanisms (CCMs) in cyanobacteria concentrates CO_2 around Rubisco and promotes cyclic electron transfer (CET) to enhance ATP production (for review, see Kaplan and Reinhold 1999; Badger and Price 2003; Price *et al.* 2008). CO_2 limitation also inhibits the repair of PSII because the increase of ROS production negatively affects the synthesis of D1 protein (reviewed in Nishiyama and Murata 2014). Similarly, high light (HL) intensities also cause an over-reduction of the photosynthetic electron carriers in the thylakoid membrane (TM) and are particularly damaging when combined with LC condition.

Apart from CCMs, different strategies are utilized by cyanobacteria in order to counteract the effects of inorganic carbon limitation and HL intensities. In particular, the up-regulation of alternative electron transfer routes dissipates the excess of electrons in ETC, thus protecting the photosystems against photodamage. Recently, the role of flavodiiron proteins (FDPs), originally called A-type flavoproteins or Flvs (Wasserfallen *et al.* 1998, Helman *et al.* 2003), has been assessed in these circumstances (Allahverdiyeva *et al.* 2011; 2013; Zhang *et al.* 2012; Bersanini *et al.* 2014; Chukhutsina *et al.* 2015).

Flavodiiron proteins are widespread among strict and facultative anaerobic bacteria and some eukaryotic protozoa, where they organize in homodimeric or homotetrameric forms (Vicente *et al.* 2008a, 2009). FDPs in these organisms function in O_2 and/or NO detoxification (Vicente *et al.* 2008b). FDPs found in cyanobacteria and some photosynthetic eukaryotes have a unique domain composition, which theoretically allows NAD(P)H oxidation to be coupled with O_2 reduction in the same enzyme. *Synechocystis* sp. PCC

***Correspondence to**: Prof. Eva-Mari Aro, Molecular Plant Biology, Department of Biochemistry, University of Turku, FI-20014, Turku, Finland. e-mail: evaaro@utu.fi*

6803 (hereafter *Synechocystis*) contains four FDPs encoded by the *sll1521* (*flv1*), *sll0219* (*flv2*), *sll0550* (*flv3*) and *sll0217* (*flv4*) genes. *In vivo*, the presence of both Flv1 and Flv3 is a prerequisite for a Mehler-like reaction occurring at downstream of PSI (Helman *et al.* 2003; Allahverdiyeva *et al.* 2013; Mustila *et al.* 2016). In this process, the Flv1 and Flv3 proteins donate electrons to O_2, similar to that in the chloroplast Mehler reaction, but, importantly, ROS are not produced in the FDP-mediated reaction (Vicente *et al.* 2002). Under inorganic carbon starvation, about 60% of the electrons deriving from PSII activity can be redirected to Flv1/Flv3-mediated Mehler-like reaction (Allahverdiyeva *et al.* 2011). The Flv1 and Flv3 proteins are particularly important in fluctuating light conditions by protecting PSI against damage (Allahverdiyeva *et al.* 2013), yet also the Flv3 homo-oligomer has a distinct but still poorly characterized role (Hackenberg *et al.* 2009; Mustila *et al.* 2016). Further, an additional copy of Flv3 present in heterocysts of *Anabaena* sp. PCC7120 (Ermakova *et al.* 2013) preserves an O_2-free environment necessary for nitrogen fixation (Ermakova *et al.* 2014). Flv1 and Flv3 homologs are also found in algae and lower plants. In *Chlamydomonas reinhardtii*, FDPs homologs facilitate the acclimation to anoxia during hydrogen photoproduction conditions (Jokel *et al.* 2015).

The *flv4-2* operon encodes Flv2 and Flv4, together with a small Sll0218 protein. Importantly, the *flv4-2* operon is highly induced in LC and HL conditions (Zhang *et al.* 2009), and it is strongly conserved in *ß*-cyanobacteria (Zhang *et al.* 2012; Allahverdiyeva *et al.* 2015). Flv4 and Flv2 proteins form a heterodimer that localizes in cytoplasm but also has a high affinity to membrane in the presence of cations (Zhang *et al.* 2012). Sll0218, the 19 kDa protein encoded by the *flv4-2* operon, locates in the membrane fraction and forms a high molecular mass complex in association with unknown partners (Zhang *et al.* 2012). The *flv4-2* operon-encoded proteins have a crucial role in photoprotection of PSII (Zhang *et al.* 2009, 2012; Bersanini *et al.* 2014). Overexpression of the *flv4-2* operon stimulates the oxidation of the PQ pool, concomitantly decreasing the production of singlet oxygen in PSII (Bersanini *et al.* 2014). Likewise, the expression of the operon increases charge separation kinetics of PSII by a slight increase of the redox potential of Q_B (Chukhutsina *et al.* 2015). Further, the deletion of the *flv4-2* operon hampers the accumulation of PSII dimers (Zhang *et al.* 2012) and a detachment of about 20% of phycobilisome antennae (Chukhutsina *et al.* 2015). Despite accumulating evidence for the photoprotective function of the *flv4-2* operon, its action mechanism is not yet clearly understood. In particular, the function of each single protein of the operon has been difficult to dissect due to the structure of the operon (order of the genes: *flv4-sll0218-flv2*). Here, with the use of different *flv4-2* operon mutants, we demonstrate that the Sll0218 protein resides in specific cell compartments where photosynthetic complexes are assembled, and it is involved in the stabilization of PSII assembly intermediates. In the absence of Sll0218, PSII assembly intermediates are accumulating, but the degradation of PSII subunits is not affected. Further, by increasing PSII stability, the Sll0218 protein is also responsible for efficient energy transfer from PBS to PSII reaction centres.

MATERIALS AND METHODS

Cyanobacterial strains and growth conditions

Wild-type (WT) *Synechocystis* sp. PCC 6803 (glucose-tolerant strain, Williams 1988) and mutant strains were grown at 30 °C in BG-11 medium (Allen 1968) supplemented with 20 mM HEPES-NaOH (pH 7.5). Cells were illuminated with white fluorescent light (L 30 W/865 Osram) with intensity of ~50 μmol photons $m^{-2} s^{-1}$ (Growth Light: GL); higher light intensities were used for other experiments (500, 1000 μmol photons $m^{-2} s^{-1}$: HL). The cultures were cultivated in Erlenmeyer flasks shaking at 120 rpm. In LC conditions, normal air was used, and Na_2CO_3 was omitted from the culture ingredients. During physiological experiments, cells were grown for 5 days starting from $OD_{750} = 0.1$ and finishing at $OD_{750} = 1.0–1.5$. Before biophysical experiments, cells were resuspended in fresh BG-11 medium and adjusted to the same chlorophyll (Chl) concentration (5 $\mu g\,mL^{-1}$ if not stated otherwise). The Chl concentration was determined in 90% methanol by absorbance measurement at 665 nm and calculated with the extinction coefficient of 78.74 $L\,g^{-1}\,cm^{-1}$ (Meeks and Castenholz 1971). The Δ*sll0218-flv2* strain was described in Helman *et al.* (2003), the Δ*flv2*, and Δ*flv4* strains in Zhang *et al.* (2012) and the OE strain in Bersanini *et al.* (2014). To create a mutant lacking only Sll0218, the Δ*sll0218-flv2* cells were transformed with self-replicating plasmid pVZ-*flagflv4* including the original *flv4* promoter region, as described in Zhang *et al.* (2012), thus introducing into cells the *flv4* gene. After complementation with *flagflv4*, the *flv2* gene was reintroduced by transformation with a plasmid (modified pPSBA2KS, Lagarde *et al.* 2000) containing the *flv2* gene under the control of the *psbA2* promoter. The *flv2* construct was integrated into the chromosome by replacing the *psbA2* gene. Deletion of the *psbA2* gene does not generally harm the cells because of concomitant adjustment of the expression of the *psbA3* gene that encodes the D1 protein identical to that encoded by the *psbA2* gene (Mohamed *et al.* 1993). To obtain the Sll0218-eYFP mutant, *sll0218* ORF together with the upstream region was amplified by PCR using FwI-*Sal*I (5'-gctcagtcgacgttcaccttctacctgggatt-3') and RvI-BamHI (5'-catgcggatcccctcctgagcctcctccaattgatggggactccttacc-3') primers followed by restriction with *Sal*I and *BamH*I. The region downstream to *sll0218* ('*sll0218* downstream') was amplified using FwII-*EcoR*I (5'-cgaccgaattcttatcttgaccatccccgct-3') and RvII-SpeI (5'-gacctactagtcaaagtaaaaacggcgatcg-3') primers followed by restriction with *EcoR*I and *Spe*I. The pEYFP-His_6-Spc^R plasmid described in Birungi *et al.* (2010) was digested in order to obtain a *Sal*I-*Spe*I vector and a *BamH*I-*EcoR*I fragment containing YFP ORF and the spectinomycin/streptomycin resistance cassette. The four fragments (*sll0218* ORF + BamHI-EcoRI fragment + *sll0218* downstream + SalI-SpeI vector) were ligated together, and the obtained pSll0218-eYFP plasmid was used for transformation of *Synechocystis* WT. A schematic map of pSll0218-eYFP plasmid is reported in Fig. S1. The

accuracy of plasmid assemblies was verified by sequencing. Segregation to homogeneity of the obtained mutants was confirmed by PCR analysis and immunoblotting.

Oxygraphic analysis by Clark-type electrode

Steady state O_2 evolution was determined with a Clark-type O_2 electrode (DW1, Hansatech) at 30 °C under saturating white light with intensity of 1000 μmol photons $m^{-2} s^{-1}$. The PSII electron transport rates were defined in the presence of an artificial electron acceptor, 2 mM 2,6-dimethyl-*p*-benzoquinone (DMBQ).

Fluorescence analysis

A pulse amplitude-modulated fluorometer Dual-PAM-100 (Walz, Effeltrich, Germany) was utilized to examine Chl fluorescence *in vivo*. Red (620 nm) actinic light was applied, and cells were stirred in 1 × 1 cm cuvettes at 30 °C during the measurements. Saturating pulses (red light, 5000 μmol photons $m^{-2} s^{-1}$, 300 ms) were used to transiently close all PSII centres. The effective yield of PSII, $Y(II) = (F_m'-F_s)/F_m'$, was measured from the cells illuminated with an actinic light intensity of 120 μmol photons $m^{-2} s^{-1}$ for 2 min.

Fluorescence emission spectra of intact cells at 77 K were determined with a USB4000-FL-450 (Ocean Optics) spectrofluorometer. The cells were frozen in liquid nitrogen directly from the GL conditions. Fluorescence emission spectra were recorded by excitation with 580 nm light obtained via interference filters 10 nm in width. Samples were adjusted to same Chl *a* concentration (5 μg mL^{-1}) before the measurements.

Protein isolation, SDS–PAGE, BN-PAGE and immunodetection

Total cell extracts as well as the soluble and membrane fractions of *Synechocystis* cells were isolated as described by Zhang *et al.* (2009, 2012). Proteins were separated by 12% (w/v) sodium dodecyl sulphate–polyacrylamide gel electrophoresis (SDS–PAGE) containing 6 M urea. Protein complexes in the membrane fractions were studied by Blue Native (BN)-PAGE, according to Zhang *et al.* (2012) using gradient polyacrylamide gels (4.5–12%). For electrophoresis in the second dimension (2D), a strip of the BN gel was incubated in the Laemmli SDS sample buffer containing 5% ß-mercaptoethanol and 6 M urea for 1 h at 25 °C. The strip was then placed onto a 1-mm-thick 12% SDS polyacrylamide gel with 6 M urea (Laemmli 1970). After electrophoresis, the proteins were transferred to a PVDF membrane (Immobilon-P; Millipore) and examined with protein-specific antibodies.

Isolation of membrane fractions

Wild-type cells were washed with 5 mM Tris buffer (pH 6.8), and resuspended in buffer I (10 mM Tris pH 6.8, 1 mM phenylmethylsulfonyl fluoride (PMSF), 600 mM sucrose, 5 mM ethylenediaminetetraaetic acid, 0.2% lysozyme). The suspension was incubated for 2 h at 30 °C and shaken; then it was washed twice in buffer II (20 mM Tris, 1 mM PMSF). Cells were disrupted with a French Press (1200 p.s.i.) followed by the treatment with DNase I (15 min at 4 °C) and centrifugation of samples (4 °C, 4500 *g*, 10 min). The obtained supernatant was adjusted to 50% sucrose, and 10 ml of this solution was overlaid with 8 ml of 39% sucrose, 6 ml of 30% sucrose and 8 ml of 10% sucrose (all in 10 mM Tris pH 6.8, 1 mM PMSF). Following centrifugation at 4 °C for 17 h at 135 000 *g*, the gradient was divided into five fractions containing 10% (I), 30% (II) or 50% (V) sucrose. To reach a higher resolution, the portion containing 39% sucrose was separated into two fractions (III and IV). The fraction V was diluted to a 20% sucrose concentration, loaded onto a linear (30% to 60%) sucrose gradient and then centrifuged for 17 h at 135 000 *g* at 4 °C, followed by fractionation and immunodetection using anti-PratA antibodies; the presence of PratA defined the PDM (PratA-defined rembrane) fractions. For more details of this procedure, see Schottkowski *et al.* (2009a).

Confocal microscopy

Fluorescence micrographs were recorded using an LSM 510 Meta confocal microscope (Carl Zeiss, Jena, Germany) with a 100x/1.4 plan apochromat oil immersion objective and an 80-μm confocal pinhole. The excitation of enhanced YFP and Chl autofluorescence were achieved respectively with the argon ion laser (514 nm) and the helium laser (543 nm). Enhanced YFP fluorescence emission was collected with a 515 nm dichroic mirror and a band pass filter of 535–590 nm. Chl autofluorescence was obtained through a 545 nm dichroic mirror and a long pass filter of 560 nm. ImageJ software was used for image analysis together with radial profile plot written by Paul Baggethun. Chl autofluorescence was used to describe the cell geometry in the determination of radial fluorescence profiles for cells. According to Sacharz *et al.* (2015), a circular area was individuated manually for each cell, and a radial distribution was determined by summing the fluorescence values at each given distance from the centre. Distributions were normalized to the cell radius.

RESULTS

Phenotype of different *flv4-2* operon mutants

Differential expression of proteins encoded by the *flv4-2* operon in mutants utilized here is shown in Fig. 1a. The Δ*flv2* mutant does not express the Flv2 protein and retained only a low amount of Flv4, whereas the Sll0218 protein accumulated to WT levels (Zhang *et al.* 2012). The Δ*sll0218-flv2* mutant lacks both Sll0218 and Flv2, and possess only a low amount of Flv4 (Zhang *et al.* 2012). Because the gene order of the *flv4-2* operon is *flv4-sll0218-flv2*, a deletion mutant of only the *sll0218* gene by direct knock out would disrupt the reading frame of the operon and compromise the expression of *flv2*, thus resulting in a strain with similar features to the Δ*sll0218-flv2* mutant. Therefore, a Δ*sll0218* mutant was generated by reintroducing *flv2* and *flv4* in the Δ*sll0218-flv2* mutant background. This led to

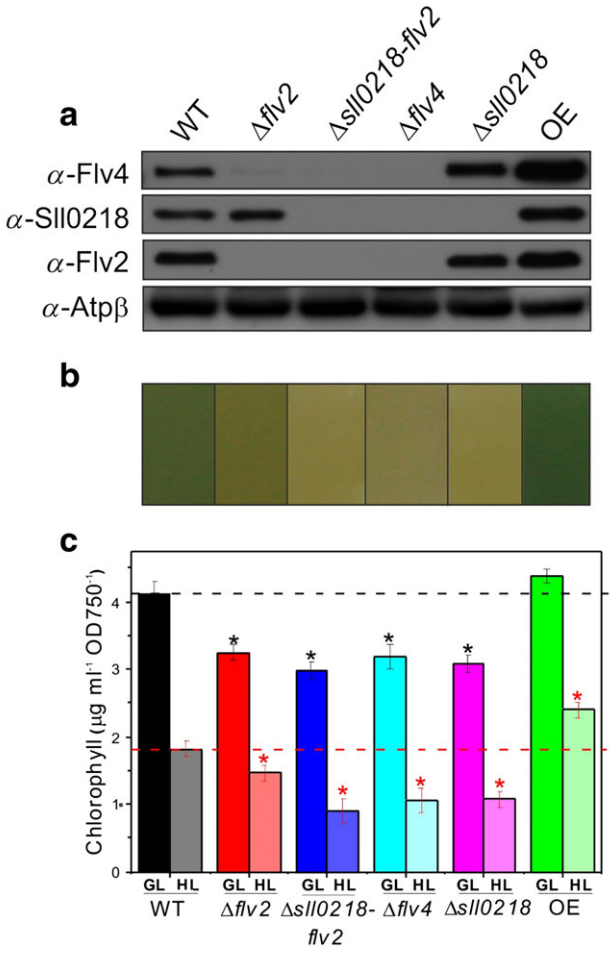

Figure 1. Phenotypes of different *flv4-2* operon mutants. (a) Immunoblot analysis of Flv4, Sll0218 and Flv2. An amount of 40 μg of proteins was loaded for each strain. (b) Colour phenotype of strains grown in high light (HL) for 6 days. (c) Chl *a* content of cultures grown in growth light (GL) and HL determined with methanol extraction and normalized to OD_{750} (means ± SD of three independent experiments). Black and red asterisks indicate statistically significant difference compared respectively with the wild-type (WT) GL values (Student's *t*-test, $P < 0.01$) and to WT HL values (Student's *t*-test, $P < 0.05$).

accumulation of the Flv2 and Flv4 proteins to a similar or slightly higher levels, respectively, compared with WT and to a concomitant absence of the Sll0218 protein. Because the Flv2/Flv2 and Flv4/Flv4 homodimers are not functional *in vivo* (Zhang *et al.* 2012), a possible excess of Flv4 in Δ*sll0218* is expected not to provide any additional effect. The OE strain showed overexpression of all three proteins, Flv4, Sll0218 and Flv2, encoded by the operon (Bersanini *et al.* 2014 Fig. 1a).

A visual phenotype of the cultures grown at 500 μmol photons $m^{-2} s^{-1}$ (HL) for 6 days is depicted in Fig. 1b: The Δ*sll0218-flv2,* Δ*flv4* and Δ*sll0218* cultures showed a distinct yellow colour compared with WT. The Δ*flv2* culture showed a mix colour phenotype between WT and the other deletion strains, whereas the OE mutant, as shown earlier in Bersanini *et al.* (2014), had a darker green colour than WT. This was reflected in the Chl *a* content of the cultures (Fig. 1c). Already in 50 μmol photons $m^{-2} s^{-1}$ (Growth Light, GL) all other mutants but not OE displayed a 20% to 25% decrease in Chl *a* content compared with WT. When cells were grown in HL, the Δ*flv2* strain displayed a similar 20–25% decrease in Chl *a* content as in GL, whereas the Δ*sll0218-flv2,* Δ*flv4* and Δ*sll0218* strains demonstrated a drop in Chl *a* content to about 50% compared with WT. The OE strain showed a 30% increase in Chl *a* content compared with WT (Fig. 1c).

Accumulation of thylakoid proteins and the PSII activity in *flv4-2* operon mutants

In GL conditions, the lack of Flv2 and reduced amount of Flv4 in the Δ*flv2* mutant were accompanied by 30% decrease of D1 content as compared with WT. The absence of the entire operon and thus all three proteins, Sll0218, Flv2 and Flv4, resulted in a 50% decrease of D1 accumulation (Δ*sll0218-flv2*, Δ*flv4*). Strikingly, the absence of only the Sll0218 protein impaired D1 accumulation to the similar extent as those lacking the whole operon-encoded proteins. Other PSII proteins (D2 and CP43) and the subunits of the Cyt b_6f and PSI complexes, the Cytf and PsaB proteins showed comparable decrease in the accumulation level as the D1 protein in the different mutant strains. On the contrary, the OE strain showed similar accumulation of thylakoid proteins as WT (Fig. 2a).

PSII functionality was determined by PAM fluorometry as Y(II) and as a rate of oxygen evolution in the presence of DMBQ, which is an artificial electron acceptor (Fig. 2b). The lack of all three proteins of the operon decreased Y(II) and O_2 evolution rate about 40–45% (Δ*sll0218-flv2,* Δ*flv4*). Importantly, the Δ*sll0218* mutant, obtained with the expression of Flv2/Flv4 in Δ*sll0218-flv2*, demonstrated only slightly lower Y (II) and PSII oxygen evolution rates (expressed on Chl *a* basis) than WT, although this difference is not statistically significant. Thus, in Δ*sll0218,* compared with Δ*sll0218-flv2*, the presence of Flv2/Flv4 rescued the activity of PSII to a large extent. The Δ*flv2* mutant possessing the Sll0218 and a faint amount of the Flv4 proteins, demonstrated about 20% and 40% lower oxygen evolution rate and Y(II), respectively, as compared with WT. In contrast, the OE mutant showed 20–40% higher PSII activity than the WT (Fig. 2b, Bersanini *et al.* 2014).

High light susceptibility of the *flv4-2* operon mutants

The sensitivity of the *flv4-2* operon mutants to HL was tested by determining the time course of inhibition of PSII oxygen evolution activity in the absence (photoinhibition) and presence of lincomycin (photodamage), an inhibitor of protein synthesis, thus blocking the PSII repair (Fig. 3). Sensitivity of the all *flv4-2* operon deletion mutants to photoinhibition was evident especially in the beginning of the shift to HL. The OE strain was more tolerant to HL than the WT in the absence (Fig. 3, Bersanini *et al.* 2014) and in the presence of lincomycin (Fig. 3). Intriguingly, only the Δ*flv2* mutant possessing the Sll0218 protein demonstrated less sensitivity to photoinhibition in the absence of lincomycin upon prolonged exposure

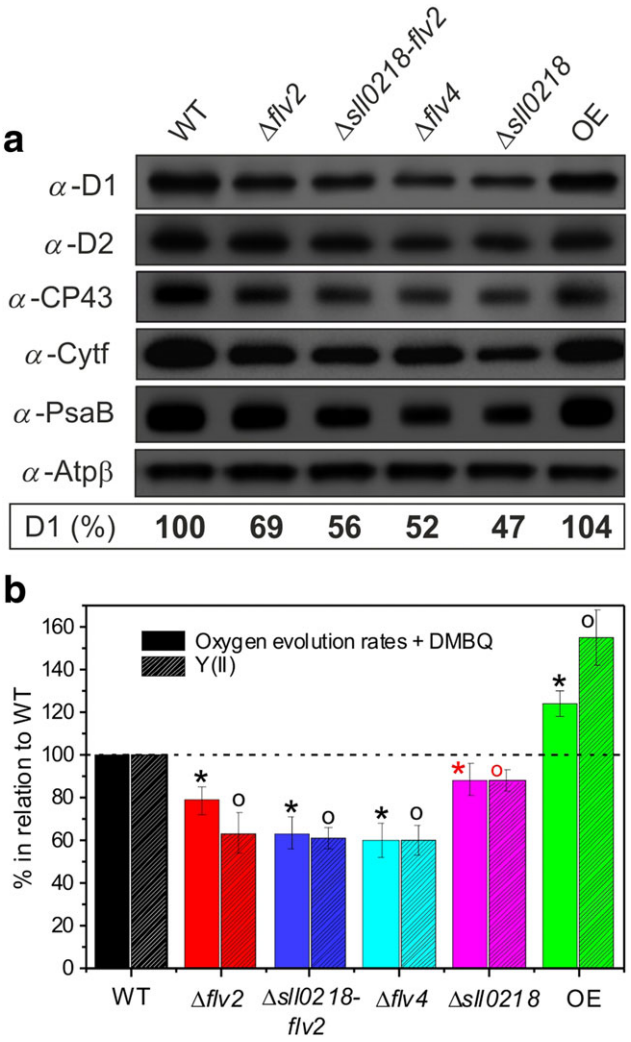

Figure 2. Accumulation of thylakoid proteins and comparison of photosystem II (PSII) activities of the *flv4-2* operon mutants. (a) Immunoblot analysis with antibodies to representative proteins of different photosynthetic complexes. The gels were loaded with 20 μg of proteins. The D1 protein quantification was performed with a GeneTool software (PerkinElmer) from three biological replicates (maximum SD of ±15%). (b) PSII activities determined as oxygen evolution rates in the presence of 2 mM 2,6-dimethyl-*p*-benzoquinone (DMBQ) with saturating light (wild-type (WT) value: 390 ± 41 μmol O_2 mg of Chl^{-1} h^{-1}), and PSII yield, Y(II), of cells exposed to red actinic light of 120 μmol photons m^{-2} s^{-1} for 2 min through PAM fluorimetry (WT value: 0.19 ± 0.02). The cultures were adjusted to same Chl concentration before the measurements. Values are means ± SD of four independent experiments. Black asterisks and black open circles: statistically significant difference of the PSII activity values of a respective strain compared with WT values (Student's *t*-test, $P < 0.05$). Red asterisk and red open circle: statistically significant difference of the PSII activity values of Δ*sll0218* strain compared with Δ*sll0218-flv2* (Student's *t*-test, $P < 0.05$).

(90 min) to HL. When the HL illumination of the cells was performed in the presence of lincomycin, differences between the mutants and WT were observed only in the beginning of the HL treatment, and disappeared after 60 min exposure of cells to HL (Fig. 3).

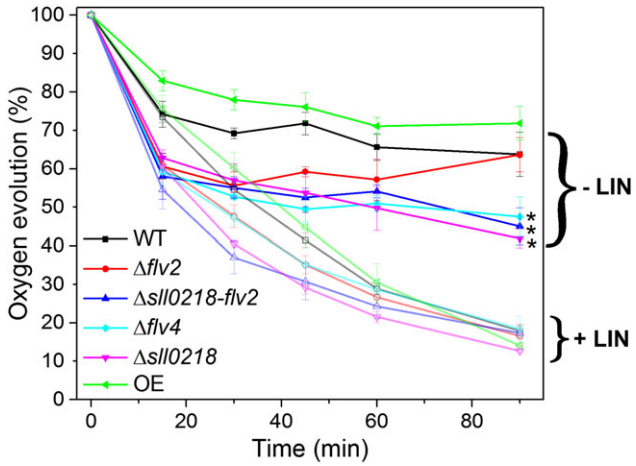

Figure 3. Time course of photosystem II photoinhibition in wild type (WT) and *flv4-2* operon mutants exposed to white light with intensity of 1000 μmol photons m^{-2} s^{-1} in the absence (−LIN) and presence (+LIN) of lincomycin (300 μg mL^{-1}). Oxygen evolution rates were measured in the presence of 2 mM 2,6-dimethyl-*p*-benzoquinone. The cultures were adjusted to a Chl concentration of 10 μg mL^{-1}. Values are means ± SD of three independent experiments. Asterisks indicate statistically significant difference of the oxygen evolution rates measured at 90 min for the Δ*sll0218-flv2*, Δ*flv4* and Δ*sll0218* strains compared to WT values (Student's *t*-test, $P < 0.05$).

The absence of Sll0218 increased PSII photosensitivity upon longer term exposure to HL, which apparently resulted from impaired PSII assembly/repair process observed only in the absence of lincomycin. Importantly, the degradation of the D1 protein, assessed in lincomycin treated cells exposed to 1000 μmol photons m^{-2} s^{-1} for a maximum of 5 h, showed no distinct pattern between the WT, Δ*sll0218-flv2* and Δ*sll0218* strains (Fig. S2), thus uncoupling the function of proteins encoded by the *flv4-2* operon from the degradation of the D1 protein.

Accumulation of PSII assembly intermediates in the *flv4-2* operon mutants

The accumulation of PSII complexes in the TM was assessed through immunoblotting of the BN-PAGE gels with D1 antibodies. Beside the PSII dimer, monomer, CP47- monomer and reaction centre (RC) complexes, the mutants lacking Sll0218, but not the Δ*flv2* mutant (Fig. S3B), showed an unusual accumulation of two small protein complexes containing the D1 protein (red arrows in Fig. 4a and Fig. S3A), with a molecular mass slightly superior to the SbtA complex. Immunoblotting of the BN-PAGE gels with antibodies specific for YCF48, a PSII assembly factor, revealed a stronger accumulation of this protein in Sll0218-lacking mutants (Fig. 4a, Fig. S3B) whereas the OE mutant demonstrated low levels of YCF48 (Fig. S3B). Noteworthy, the two closely migrating YCF48 complexes in the BN-PAGE co-migrated with the D1-containing complexes mentioned in the preceding texts. Next, this region of protein complexes, indicated by a red rectangle in the first BN-gel of Fig. 4a, was subjected to SDS–PAGE in the 2D followed by immunoblotting

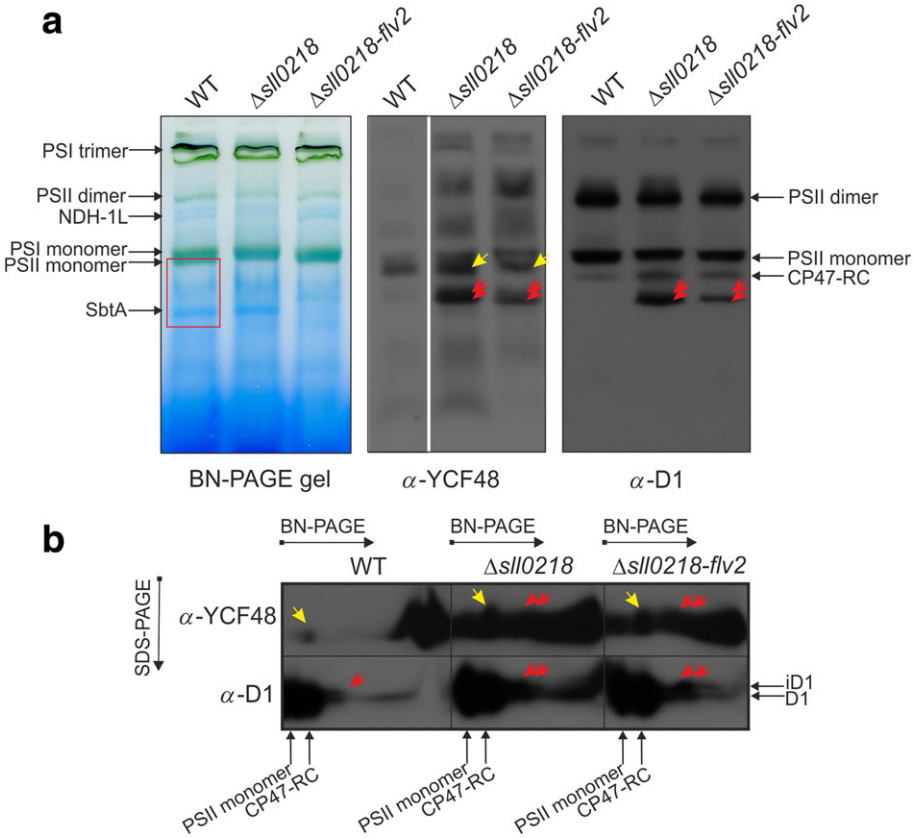

Figure 4. Accumulation of photosystem II (PSII) intermediates in wild type (WT), Δ*sll0218* and Δ*sll0218-flv2* strains. (a) The Blue Native polyacrylamide gel electrophoresis (BN-PAGE) gel was loaded with 100 μg of proteins and analysed by further immunoblotting with D1 and YCF48 antibodies. The yellow arrows indicate the reaction centre (RC*) complex identified by Komenda *et al.* (2008) and Rengstl *et al.* (2013). The red arrows indicate protein complexes that accumulate in Δ*sll0218* and Δ*sll0218-flv2* strains, and possibly correspond to the PSII RCa complex forms demonstrated by (Komenda *et al.* 2008). (b) Protein complexes from the red rectangle indicated in the BN-gel in A were run by sodium dodecyl sulphate (SDS)–PAGE in the second dimension and immunoblotted with D1 and YCF48 antibodies. The complexes indicated in (a) by yellow and red arrows were identified by immunoblotting with D1 and YCF48 antibodies and are indicated with similar arrows in (b). The intermediate form of D1 (iD1) could also be identified in the complexes.

with D1 and YCF48 antibodies. This analysis showed that YCF48 and D1 indeed belong to the same PSII intermediate complex (Fig. 4b). The PSII subcomplex indicated by a yellow arrow likely represents the RC* (PSII reaction centre complex *), localized between the CP43-less PSII monomer (CP47-RC) and PSII monomeric complexes (Fig, 4, Fig. S3B, Rengstl *et al.* 2013). RC* is composed of full D1 or its intermediate form (iD1), D2, PsbI, cytb$_{559}$, YCF48, together with a Ycf39-HliD subcomplex (Komenda *et al.* 2008; Knoppová *et al.* 2014). The two small PSII subcomplexes identified in the Sll0218-lacking mutants and indicated by red arrows in Fig. 4, possibly correspond to the RCa complexes, which is a RC* devoid of Ycf39-HliD subcomplex (Knoppová *et al.* 2014). These complexes could not be visualized with protein staining, most probably because of their low relative abundance.

PSII assembly factors in the *flv4-2* operon mutants

Because the assembly of PSII seemed to be malfunctioning in the *flv4-2* operon mutants, the content of a number of proteins involved in PSII assembly was next addressed by immunoblotting with corresponding antibodies. As already suggested by the BN-PAGE gels (Fig. 4), the most conspicuous differences between the *flv4-2* operon mutants existed in the amounts of the YCF48 protein. In comparison with WT, the absence of Sll0218 increased the content of YCF48 to maximum of 140%, while the OE strain had only about 50% of WT YCF48 level (Fig. 5a). The amount of the Sll0933 protein, a homolog of plant PAM68 (Armbruster *et al.* 2010), which was reported to interact with YCF48 (Rengstl *et al.* 2013), did not differ significantly among the *flv4-2* operon mutants. Similar constancy was observed for PratA (Fig. 5a), which is responsible for the delivery of Mn^{2+} ions to the precursor form of D1 (pD1) protein (Stengel *et al.* 2012). The levels of protochlorophyllide oxidoreductase (POR), a protein involved in Chl biosynthesis (Schottkowski *et al.* 2009a), were slightly elevated in all the mutants. The protein levels of Pitt, a membrane-bound tetratricopeptide repeat protein that binds and stabilizes POR (Schottkowski *et al.* 2009b), and Vipp1, involved in TM maintenance (Westphal *et al.* 2001), were slightly lower in the *flv4-2* operon deletion mutants, compared with WT. The levels of Oxa1 protein, which supports

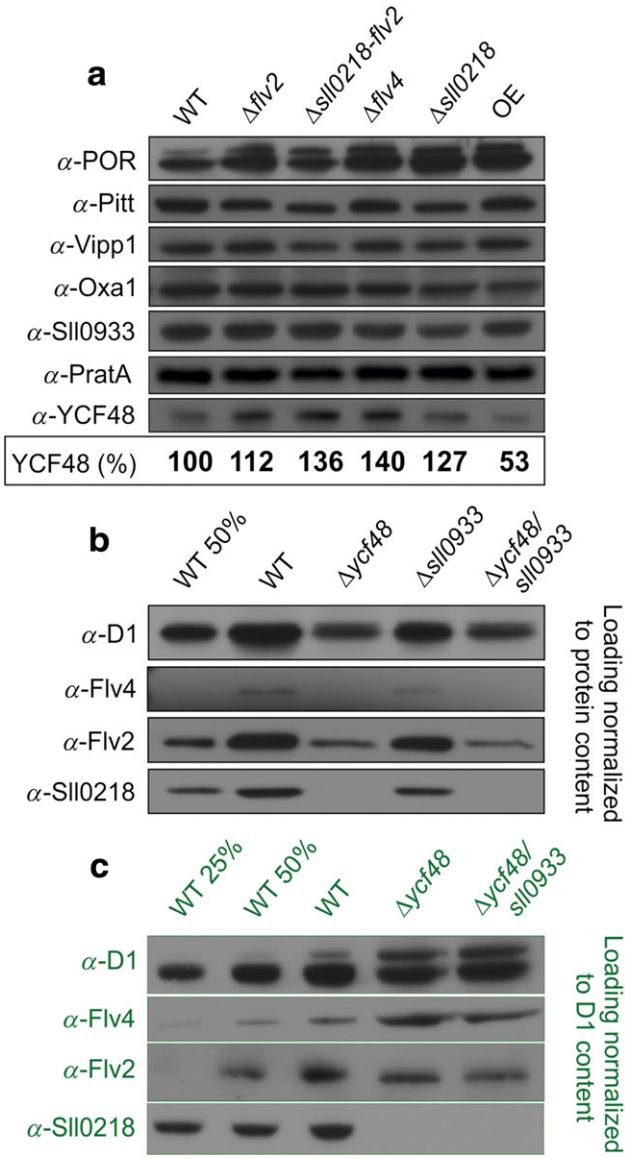

Figure 5. (a) Immunoblot demonstrating the accumulation of different photosystem II assembly-related factors in the *flv4-2* operon mutants (see details in the text). The gels were loaded with 20 μg of proteins. The YCF48 protein quantification was achieved with a GeneTool (PerkinElmer) software from three biological replicates (maximum SD of ±15%). (b) Accumulation of *flv4-2* operon-encoded proteins in wild type (WT), Δ*ycf48*, Δ*sll0933* and Δ Δ*ycf48/sll0933* strains detected by immunoblotting the gels loaded with 20 μg of protein. (c) Accumulation of *flv4-2* operon-encoded proteins in WT, Δ*ycf48* and Δ*ycf48/sll0933* strains detected by immunoblotting the gels loaded with an amount of protein normalized to the D1 content, making use of the quantification of D1 content obtained in (b).

the integration, folding, and/or assembly of precursor D1 form (Ossenbühl *et al.* 2006), were slightly lower in the OE mutant (Fig. 5a). The accumulation of a stomatin-like protein homolog, called Phb3 (Slr1128), with unclear function in cyanobacteria, was impaired in Sll0218-lacking mutants (Fig. S4).

Presence of *flv4-2* operon-encoded proteins in *ycf48* and *sll0933* deletion mutants

Because the presence of PSII assembly factors differs among the *flv4-2* operon mutants, the reverse situation was also tested by assessing the contents of the *flv4-2* operon-encoded proteins in Δ*ycf48*, Δ*sll0933* and the double mutant Δ*ycf48/sll0933*. When the loading of gels was normalized to the total protein content, the D1 amounts were, as expected, lower in the PSII assembly mutants than in WT (Fig. 5b, Komenda *et al.* 2008; Rengstl *et al.* 2013). Nevertheless, we could detect all the *flv4-2* operon-encoded proteins in the Δ*sll0933* mutant. In the mutants lacking YCF48, only Flv2 was detectable; Flv4 was difficult to identify possibly because of the lower quality of the antibody, but the Sll0218 protein was clearly absent (Fig. 5b). More detailed characterization of the expression of the *flv4-2* operon encoded proteins was performed in the Δ*ycf48* and Δ*ycf48/sll0933* strains.Because the function of the *flv4-2* operon-encoded proteins is related to PSII, the loading of proteins in the gels was normalized to the D1 content, according to the quantification performed in the previous experiment. With this setup, the Flv2 and Flv4 proteins could be clearly identified. Interestingly, the Sll0218 protein still remained undetected (Fig. 5c).

Localization of Sll0218 in *Synechocystis* cells

To investigate the subcellular localization of the Sll0218 protein *in vivo*, the yellow fluorescent protein (YFP) was fused to the C-terminus of Sll0218. Subsequent immunoblottings with the Sll0218 and YFP specific antibodies confirmed the expression of the Sll0218-YFP protein, with an approximate size of ~50 KDa (Fig. S5). Confocal fluorescence microscopy images revealed distribution of Sll0218-YFP in small spots in the cells (Fig. 6a). The number of spots was determined to be in an average of 2.13 per cell (Fig. 6b). Further comparison with the radial distributions of Chl fluorescence and Sll0218-YFP fluorescence showed that Sll0218 spots were localized mainly at the peripheral side of the Chl fluorescence patterns (Fig. 6c), thus denoting the localization of the fusion proteins to the side of TM which is more in the vicinity to the cytoplasmic membrane (Mullineaux and Sarcina 2002).

To further explore Sll0218 localization, *Synechocystis* membranes were isolated and fractionated according to Rengstl *et al.* (2011) and the PratA-defined membrane areas, called PDMs, were defined. PDMs are considered to be specific areas of biogenesis of photosynthetic complexes, in particular of PSII, and are located in the contact area of the TM with the cytoplasmic membrane, or around the thylakoid biogenesis centres (Stengel *et al.* 2012). The protein content of the PDM fraction was verified by immunoblotting with PratA, D1, PsaB, YCF48 and Sll0933 antibodies and demonstrated a typical pattern with PratA strictly accumulated in PDM fractions, D1 and YCF48 accumulated in PDM and TM fractions, while PsaB and Sll0933 represented strict TM markers (Rengstl *et al.* 2011). Most importantly, the Sll0218 protein was present only in the PDM fractions (Fig. 6d).

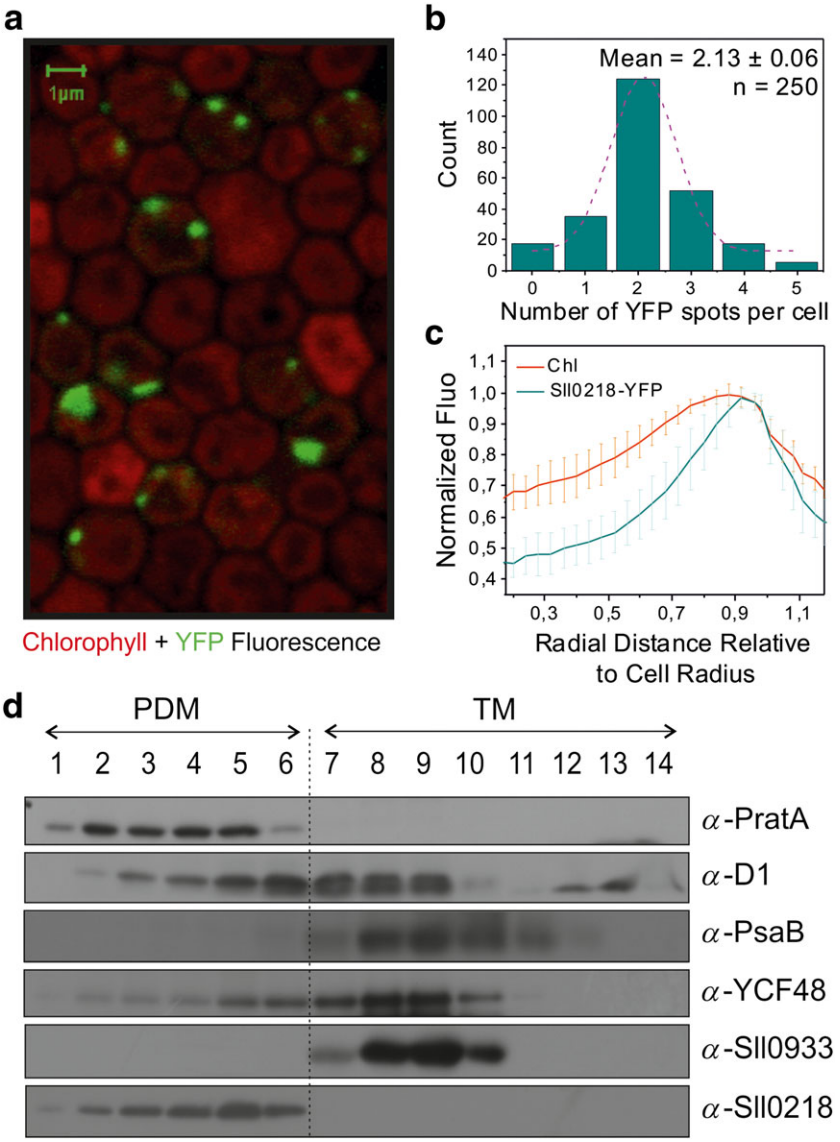

Figure 6. Localization of the Sll0218 protein. (a) A confocal fluorescence image of *Synechocystis* Sll0218-YFP cells, showing merged YFP fluorescence with chlorophyll fluorescence (YFP in green, chlorophyll in red) for cells grown in growth light. (b) Sll0218-YFP spot numbers per cell ± SEM ($n = 250$). (c) Averaged fluorescence radial distributions ($n = 30$) normalized to cell radius. Red lines indicate chlorophyll fluorescence profile ± SD, blue lines indicate YFP fluorescence profile ± SD. (d) Localization of Sll0218 in the PDM fraction. *Synechocystis* cell extracts of the wild-type strain were separated by two consecutive rounds of sucrose density gradient centrifugation. The second linear gradient from 20% to 60% sucrose was divided into 14 fractions followed by immunoblotting with indicated antibodies. Fractions 1–6 represent PDMs, fractions 7–14 represent thylakoid membranes (TMs). Sample volumes were normalized to the volume of fraction 7 that contained 40 μg of protein.

Differences in light harvesting properties of the *flv4-2* operon mutants

To distinguish the role of *flv4-2* operon-encoded different proteins in harvesting of light energy, we recorded the fluorescence emission spectra at 77 K, with an excitation at 580 nm. High F685 peak clearly distinguished the Δ*flv4* and Δ*sll0218-flv2* strains from WT, as reported also earlier (Zhang *et al.* 2012; Bersanini *et al.* 2014). Nevertheless, the Δ*sll0218* strain also demonstrated a high F685 as compared with WT, while the Δ*flv2* strain, expressing the Sll0218 protein, had just a slightly higher F685 peak compared with that in WT.

Moreover, the minimal level of the fluorescence in the dark, the F_0, which is also an indication of antenna detachment (Campbell *et al.* 1998; Acuña *et al.* 2015), was clearly higher in the Sll0218-lacking mutants (Fig. S6), thus confirming that the lack of Sll0218 is the main cause for antenna detachment.

DISCUSSION

Although the research on FDPs in oxygenic photosynthetic organisms is constantly increasing, several fundamental questions on their mode of action and reasons for arrangement in an

operon still remain unclear. This is particularly the case with the *flv4-2* operon-encoded proteins and their function in photoprotection of cyanobacterial PSII (Zhang *et al.* 2009, 2012; Hakkila *et al.* 2013; Bersanini *et al.* 2014; Chukhutsina *et al.* 2015). In this work, we addressed the function of the three proteins encoded by the *flv4-2* operon, the Flv4, Sll0218 and Flv2 proteins. Towards this end, we characterized different *flv4-2* operon mutants with deficiencies or overexpression of Flv2, Sll0218 and Flv4 proteins, together or singularly, and assessed their specific significance for the functionality and turnover of PSII.

Sll0218 contributes to stabilization of newly assembled PSII in thylakoid biogenesis centres

The Sll0218 protein encoded by the *flv4-2* operon has remained the most cryptic component of this photoprotection machinery. The partially independent function of Sll0218 from the Flv2/4 heterodimer can already be deduced from the expression pattern of the Flv2, Sll0218 and Flv4 proteins in the mutant collection used here. When the *flv2* gene is deleted (Δ*flv2* strain), also the expression of the Flv4 protein is low, but the Sll0218 protein is present at WT-levels (Fig. 1a). Conversely, in mutants lacking YCF48, the Flv2 and Flv4 proteins are present but the Sll0218 protein is missing (Fig. 5b,c). Thus, it is highly conceivable that the presence of YCF48 is required for the specific accumulation of Sll0218. Additionally, both are membrane proteins with reported connections to PSII (Komenda *et al.* 2008; Zhang *et al.* 2012; Mabbitt *et al.* 2014; Chukhutsina *et al.* 2015). These observations prompted us to investigate in more detail the role of the Sll0218 protein as a distinct component and separate player from that of the Flv2/Flv4 heterodimer in protection of PSII.

The fact that the lack of the sole Sll0218 protein (Δ*sll0218*) caused, under LC growth conditions, a similar deficiency in Chl *a*, PSII and other photosynthetic complexes as observed in the entire *flv4-2* operon deletion mutants (50% less PSII than in WT on protein basis) (Fig. 1c) suggested a before unforeseen role for the Sll0218 protein. Despite the scarcity of PSII proteins in the absence of Sll0218, they seemed to be properly assembled as the Δ*sll0218* mutant displayed nearly WT-like PSII activity when expressed on the Chl basis. No significant compromise in the functionality of PSII in the *sll0218* mutant suggested that Sll0218 may rather play a role in stabilization of PSII under repair/assembly.

To test the hypothesis of a PSII stabilization role for Sll0218, *Synechocystis flv4-2* operon mutants were shifted to HL in order to enhance PSII photoinhibition and subsequent PSII repair/assembly processes. Indeed, the mutants that lacked Sll0218 were the most sensitive to photoinhibition, as also indicated by drastic changes in the colour and the Chl *a* content of the cultures (Fig. 1b,c). When lincomycin was added to the cells upon exposure to HL, all *flv4-2* operon mutants displayed similar PSII inhibition kinetics from 60 min illumination onwards. Collectively, the photoinhibition experiments in the absence and presence of lincomycin support the hypothesis of the role of Sll0218 protein in the stabilization of assembly/repair of PSII. The PSII repair starts with degradation of the damaged D1 protein (Aro *et al.* 1993; Aro *et al.* 2005). This initial PSII repair phase, however, did not reveal any significant differences between the mutants. (Fig. S2), suggesting that the proteolytic degradation of D1 is not considerably affected by the presence or absence of Sll0218. Subsequent steps of PSII repair involve a co-translational incorporation of the D1 protein into partially disassembled PSII complex and subsequent reassembly of the detached proteins and cofactor components (Aro *et al.* 2005; Järvi *et al.* 2015). These assembly/repair phases of PSII have been investigated in cyanobacteria in great detail during the past few years (see reviews Komenda *et al.* 2012; Nickelsen and Rengstl 2013; Heinz *et al.* 2016).

Characterization of the *flv4-2* operon mutants with respect to PSII assembly/repair revealed two intermediate complexes containing D1 and YCF48, which specifically accumulated in the strains lacking the Sll0218 protein (Fig. 4). According to the mobility in the BN-PAGE gels, these PSII subcomplexes could represent two distinct forms of the PSII RCa complex identified by Komenda *et al.* (2008). The YCF48 protein was present in high amounts in mutants lacking the Sll0218 protein. YCF48 is an important PSII assembly factor that optimizes the assembly of the RC complex by stabilizing the newly synthesized pD1 and its following interaction with the D2-Cyt b_{559} complex (Komenda *et al.* 2008). Likewise, YCF48 contributes to the replacement of the damaged D1 during the PSII repair process (Komenda *et al.* 2008). The localization of YCF48 to both the PDM fractions and TM fractions (Fig. 6d and Rengstl *et al.* 2011) correlates with its role in both PSII assembly and repair. Differences in the early assembly steps are likely reflected in poor accumulation of PSII dimers in the absence of Sll0218 (Zhang *et al.* 2012), and conversely, in relatively low amounts of CP47-RC assembly intermediate complexes in the *flv4-2* operon OE mutant (Chukhutsina *et al.* 2015). The PSII assembly problems and accumulation of PSII-YCF48 assembly intermediates, occurring specifically in the absence of Sll0218, suggest a key role for the Sll0218 protein in stabilization of the early PSII assembly intermediates and consequently also for the formation and accumulation of PSII monomer and dimer complexes.

Interestingly, Δ*sll0218-flv2* and Δ*sll0218* mutants also revealed an impaired accumulation of a stomatin-like protein, called Phb3, which forms a ring-like assembly with a diameter of ~16 nm (Boehm *et al.* 2009) and has been localized to the PSII repair zones of the membrane (Sacharz *et al.* 2015). Proteins of the stomatin family might have a scaffold function in the organization of the membrane (Browman *et al.* 2007). Cyanobacterial thylakoid biogenesis centres, with particular focus on PSII assembly and repair, have been under extensive research during the past 10 years (van de Meene *et al.* 2006; Rengstl *et al.* 2011; Stengel *et al.* 2012; Heinz *et al.* 2016). Localization of Sll0218 by confocal microscopy to definite spots at the peripheral side of TM (Fig. 6a,b,c) together with independent membrane fractionation studies (Fig. 6d) that selectively detected the Sll0218 protein in the PDM fractions provided compelling evidence that the Sll0218 protein is an integral component of the thylakoid biogenesis centres. Interestingly, Sll0218 specifically localizes to PDM fractions while YCF48 localizes to both PDM and TM fractions, probably suggesting a

role of Sll0218 in the stabilization of early stages of PSII assembly, while YCF48 is likely to act in both the assembly and repair processes (Komenda *et al.* 2008).

In some cases, the fusion of a relatively small hydrophobic protein to a much larger hydrophilic YFP could hamper its mobility with a possibility that the fusion product is found exclusively at the periphery of the cell, whereas the native functional protein is localized differently. However, Sll0218 is localized to the membrane fraction, and it forms a high molecular mass complex that can be detected by immunoblotting of native gels loaded with the membrane extract of *Synechocystis* cells (Zhang *et al.* 2012). Therefore, in accordance with the membrane fractionation studies (Fig. 6d) that put Sll0218 in the PDM fractions (PDM areas localize at the periphery of the cells as shown by immunogold labelling by Stengel *et al.* 2012), it is unlikely that the observed Sll0218-YFP fluorescence from the membrane region of the cells would be an artefact.

The lack of Sll0218 also has indirect consequences observed as phycobilisome antenna detachment. This phenomenon was previously reported in *flv4-2* operon mutants, together with a concomitant relative decrease of PSII dimers in the Δ*flv4* mutant (Chukhutsina *et al.* 2015). The phycobilisome detachment in the *flv4-2* operon mutants was visualized by an increase of the F685 peak in steady-state fluorescence emission spectra at 77 K (Zhang *et al.* 2012; Bersanini *et al.* 2014), and the effect was proposed to be related to the lack of Sll0218, as a consequence of PSII dimer destabilization (Chukhutsina *et al.* 2015). This assumption, however, lacked direct evidence in the absence of suitable mutants for experimentation. Use of the Δ*sll0218* mutant finally provided direct proof and indicated that the enhanced 77 K fluorescence emission at F685 results from the absence of Sll0218 (Fig. 7). Thus, the absence of Sll0218, via destabilization of PSII, is responsible also for the antenna detachment.

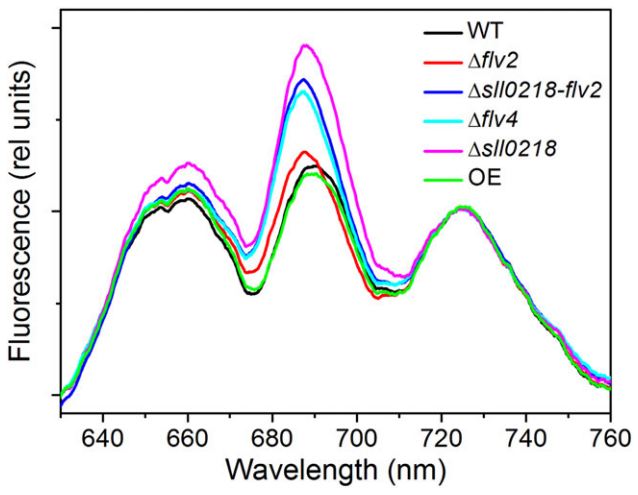

Figure 7. The 77 K steady-state fluorescence emission spectra of the *flv4-2* operon mutants induced by excitation with 580-nm light. The spectra were averaged from at least three independent experiments. Each spectrum was normalized to photosystem I fluorescence peak at 723 nm.

Concerted action of Flv2/Flv4 and Sll0218 enables efficient PSII accumulation and function

The expression of the Flv2 and Flv4 proteins, and their function as an Flv2/Flv4 heterodimer, is a prerequisite for the maintenance of PSII activity, as evidenced by the fact that the *flv4-2* operon mutants Δ*flv2,* Δ*sll0218-flv2 and* Δ*flv4* display malfunction of PSII electron transfer (Fig. 2b). Conversely, the absence of the Sll0218 protein (Δ*sll0218*) (Fig. 2b) did not affect the functionality of existing PSII centres but severely destabilized the early assembly/repair intermediates of PSII. Thus, the dual role of the *flv4-2* operon encoded proteins in turnover of the PSII centres, firstly by alleviating the electron pressure in the ETC (Flv2/Flv4) and, secondly, by providing stability for PSII early assembly intermediates (Sll0218) calls for coordinated expression of the proteins in the operon. Strong transcriptional regulation of the operon by antisense RNAs (Eisenhut *et al.* 2012) guarantees controlled expression of the operon when environmental conditions change and PSII needs efficient protection. Both protection mechanisms are important for optimal maintenance of PSII under ambient CO_2 levels.

Maintenance of PSII centres even in GL, as deduced from the amount of the D1 protein, is severely impaired in the absence of Sll0218 (50% less than in WT), while in the absence of Flv2/Flv4 the D1 protein accumulation is less compromised, only by about 30% (Fig. 2a; Zhang *et al.* 2012). As demonstrated by the Δ*sll0218* mutant, the function of Flv2/Flv4 in alleviation of electron accumulation in ETC only partially helps in keeping the PSII complexes at optimal level. In GL, the presence of Flv2/Flv4 in the Δ*sll0218* mutant significantly improved the maintenance of PSII activity compared to the Δ*sll0218-flv2* mutant, whereas at HL the presence of Flv2/Flv4 failed to rescue the photosensitive phenotype, as happened also for Δ*sll0218-flv2* and Δ*flv4* (Fig. 3). Thus, the exposure of cells to increasing light intensities, with concomitant enhancement of the PSII assembly/repair cycle, makes Sll0218 the most indispensable protein encoded by the *flv4-2* operon.

ACKNOWLEDGMENTS

This work was supported by the Alfred Kordelin Foundation and by the Academy of Finland Projects (N° 271832; N° 273870; N° 272424). The following projects are also acknowledged: PHOTOCOMM (ITN, 317184), CALIPSO (ITN, 607607), TEKES (LIF 40128/14), NKFI-H (NN-110960), and SOLARH2 (N° 212508). Work in the Nickelsen lab was supported by the DFG Research Unit FOR2092 (Ni390/9) and by LMU Munich's Institutional Strategy LMUexcellent within the framework of the German Excellence Initiative. Dr J. Komenda is acknowledged for sharing the Δ*ycf48* and Δ*ycf48/sll0933* strains.

CONFLICT OF INTEREST

The authors declare no conflict of interest.

REFERENCES

Acuña A.M., Snellenburg J.J., Gwizdala M., Kirilovsky D., van Grondelle R. & van Stokkum I.H. (2015) Resolving the contribution of the uncoupled phycobilisomes to cyanobacterial pulse-amplitude modulated (PAM) fluorometry signals. *Photosynthesis Research* **127**, 91–102.

Allahverdiyeva Y., Ermakova M., Eisenhut M., Zhang P., Richaud P., Hagemann M.,…, Aro EM. (2011) Interplay between flavodiiron proteins and photorespiration in *Synechocystis* sp. PCC 6803. *Journal of Biological Chemistry* **286**: 24007–24014.

Allahverdiyeva Y., Isojarvi J., Zhang P. & Aro EM. (2015) Cyanobacterial oxygenic photosynthesis is protected by flavodiiron proteins. *Life* **5**: 716–743.

Allahverdiyeva Y., Mustila H., Ermakova M., Bersanini L., Richaud P., Ajlani G. …, Aro EM. (2013) Flavodiiron proteins Flv1 and Flv3 enable cyanobacterial growth and photosynthesis under fluctuating light. *Proceedings of the National Academy of Sciences USA* **110**, 4111–4116.

Allen M.M. (1968) Simple conditions for growth of unicellular blue-green algae on plates. *Journal of Phycology* **4**: 1–4.

Armbruster U., Zühlke J., Rengstl B., Kreller R., Makarenko E., Rühle T.…, Leister D. (2010) The *Arabidopsis* thylakoid protein PAM68 is required for efficient D1 biogenesis and photosystem II assembly. *The Plant Cell* **22**, 3439–3460.

Aro E.M., Virgin I. & Andersson B. (1993) Photoinhibition of photosystem II. Inactivation, protein damage and turnover. *Biochimica et Biophysica Acta* **1143**, 113–134.

Aro E.M., Suorsa M., Rokka A, Allahverdiyeva Y., Paakkarinen V., Saleem A.…, Rintamäki E. (2005) Dynamics of photosystem II: a proteomic approach to thylakoid protein complexes. *Journal of Experimental Botany* **56**, 347–356.

Badger M.R. & Price G.D. (2003) CO_2 concentrating mechanisms in cyanobacteria: molecular components, their diversity and evolution. *Journal of Experimental Botany* **54**, 609–622.

Birungi M., Folea M., Battchikova N., Xu M., Mi H., Ogawa T.…, Boekema E.J. (2010) Possibilities of subunit localization with fluorescent protein tags and electron microscopy examplified by a cyanobacterial NDH-1 study. *Biochimica et Biophysica Acta* **1797**, 1681–1686.

Boehm M., Nield J., Zhang P., Aro E.M., Komenda J. & Nixon P.J. (2009) Structural and mutational analysis of band 7 proteins in the cyanobacterium *Synechocystis* sp strain PCC 6803. *Journal of Bacteriology* **191**, 6425–6435.

Bersanini L., Battchikova N., Jokel M., Rehman A., Vass I., Allahverdiyeva Y. & Aro E.M. (2014) Flavodiiron protein Flv2/Flv4-related photoprotective mechanism dissipates excitation pressure of PSII in cooperation with phycobilisomes in cyanobacteria. *Plant Physiology* **164**, 805–818.

Browman D.T., Hoegg M.B. & Robbins S.M. (2007) The SPFH domain-containing proteins: more than lipid raft markers. *Trends in Cell Biology* **17**, 394–402.

Campbell D., Hurry V., Clarke A.K., Gustafsson P. & Oquist G. (1998) Chlorophyll fluorescence analysis of cyanobacterial photosynthesis and acclimation. *Microbiology and Molecular Biology Reviews* **62**, 667–683.

Chukhutsina V., Bersanini L., Aro E.M. & van Amerongen H. (2015) Cyanobacterial *flv4-2* operon-encoded proteins optimize light-harvesting and charge separation in photosystem II. *Molecular Plant* **8**, 747–761.

Eisenhut M., Georg J., Klähn S., Sakurai I., Mustila H., Zhang P.…, Aro EM. (2012) The antisense RNA As1_flv4 in the cyanobacterium *Synechocystis* sp. PCC 6803 prevents premature expression of the *flv4-2* operon upon shift in inorganic carbon supply. *Journal of Biological Chemistry* **287**, 33153–33162.

Ermakova M., Battchikova N., Allahverdiyeva Y. & Aro E.M. (2013) Novel heterocyst-specific flavodiiron proteins in *Anabaena* sp. PCC 7120. *FEBS Letters* **587**, 82–87.

Ermakova M., Battchikova N., Richaud P., Leino H., Kosourov S., Isojärvi J.…, Aro EM. (2014) Heterocyst-specific flavodiiron protein Flv3B enables oxic diazotrophic growth of the filamentous cyanobacterium *Anabaena* sp. PCC 7120. *Proceedings of the National Academy of Sciences USA* **111**, 11205–11210.

Hackenberg C., Engelhardt A., Matthijs H.C., Wittink F., Bauwe H., Kaplan A. & Hagemann M. (2009) Photorespiratory 2-phosphoglycolate metabolism and photoreduction of O_2 cooperate in high-light acclimation of *Synechocystis* sp. strain PCC 6803. *Planta* **230**, 625–637.

Hakkila K., Antal T., Gunnelius L., Kurkela J., Matthijs H.C.P., Tyystjärvi E. & Tyystjärvi T. (2013) Group 2 sigma factor mutant ΔsigCDE of the cyanobacterium *Synechocystis* sp. PCC 6803 reveals functionality of both carotenoids and flavodiiron proteins in photoprotection of photosystem II. *Plant and Cell Physiology* **54**, 1780–1790.

Heinz S., Liauw P., Nickelsen J. & Nowaczyk M. (2016) Analysis of photosystem II biogenesis in cyanobacteria. *Biochimica et Biophysica Acta* **1857**, 274–287.

Helman Y., Tchernov D., Reinhold L., Shibata M., Ogawa T., Schwarz R.…, Kaplan A. (2003) Genes encoding A-type flavoproteins are essential for photoreduction of O_2 in cyanobacteria. *Current Biology* **13**, 230–235.

Järvi S., Suorsa M. & Aro E.M. (2015) Photosystem II repair in plant chloroplasts – regulation, assisting proteins and shared components with photosystem II biogenesis. *Biochimica et Biophysica Acta* **1847**(9), 900–909.

Jokel M., Kosourov S., Battchikova N., Tsygankov A.A., Aro E.M. & Allahverdiyeva Y. (2015) *Chlamydomonas* flavodiiron proteins facilitate acclimation to anoxia during sulfur deprivation. *Plant and Cell Physiology* **56**, 1598–1607.

Kaplan A. & Reinhold L. (1999) CO_2 concentrating mechanisms in photosynthetic microorganisms. *Annual Reviews in Plant Physiology and Plant Molecular Biology* **50**, 539–570.

Knoppová J., Sobotka R., Tichý M., Yu J., Konik P., Halada P.…, Komenda J. (2014) Discovery of a chlorophyll binding protein complex involved in the early steps of photosystem II assembly in *Synechocystis*. *The Plant Cell* **26**, 1200–1212.

Komenda J., Nickelsen J., Tichy M., Prasil O., Eichacker L.A. & Nixon P.J. (2008) The cyanobacterial homologue of HCF136/YCF48 is a component of an early photosystem II assembly complex and is important for both the efficient assembly and repair of photosystem II in *Synechocystis* sp. PCC 6803. *Journal of Biological Chemistry* **283**, 22390–99.

Komenda J., Sobotka R. & Nixon P.J. (2012) Assembling and maintaining the photosystem II complex in chloroplasts and cyanobacteria. *Current Opinion in Plant Biology* **15**, 245–251.

Laemmli U.K. (1970) Cleavage of structural proteins during the assembly of the head of bacteriophage T4. *Nature* **227**, 680–685.

Lagarde D., Beuf L. & Vermaas W. (2000) Increased production of zeaxanthin and other pigments by application of genetic engineering techniques to *Synechocystis* sp. strain PCC 6803. *Applied Environmental Microbiology* **66**, 64–72.

Mabbitt P.D., Wilbanks S.M. & Eaton-Rye J.J. (2014) Structure and function of the hydrophilic Photosystem II assembly proteins: Psb27, Psb28 and Ycf48. *Plant Physiology and Biochemistry* **81**, 96–107.

Mackenzie T.D., Burns R.A. & Campbell D.A. (2004) Carbon status constrains light acclimation in the cyanobacterium *Synechococcus elongatus*. *Plant Physiology* **136**, 3301–3312.

Meeks J.C. & Castenholz R.W. (1971) Growth and photosynthesis in an extreme thermophile *Synechococcus lividus* (Cyanophyta). *Archives fur Mikrobiologie* **78**, 25–41.

Mohamed A., Eriksson J., Osiewacz H.D. & Jansson C. (1993) Differential expression of the *psbA* genes in the cyanobacterium *Synechocystis* 6803. *Molecular and General Genetics MGG* **238**, 161–168.

Mullineaux C.W. & Sarcina M. (2002) Probing the dynamics of photosynthetic membranes with fluorescence recovery after photobleaching. *Trends in Plant Science* **7**, 237–240.

Mustila H., Paananen P., Battchikova N., Santana-Sanchez A., Muth-Pawlak D., Hagemann M.…, Allahverdiyeva Y. (2016) The flavodiiron protein Flv3 functions as a homo-oligomer during stress acclimation and is distinct from the Flv1/Flv3 hetero-oligomer specific to the O2 photoreduction pathway. *Plant and Cell Physiology* doi:10.1093/pcp/pcw047.

Nickelsen J. & Rengstl B. (2013) Photosystem II assembly: from cyanobacteria to plants. *Annual Reviews in Plant Biology* **64**, 609–635.

Nishiyama Y. & Murata N. (2014) Revised scheme for the mechanism of photoinhibition and its application to enhance the abiotic stress tolerance of the photosynthetic machinery. *Applied Microbiology and Biotechnology* **98**, 8777–8796.

Ossenbühl F., Inaba-Sulpice M., Meurer J., Soll J. & Eichacker L.A. (2006) The *Synechocystis* sp PCC 6803 Oxa1 homolog is essential for membrane integration of reaction center precursor protein pD1. *The Plant Cell* **18**, 2236–2246.

Price G.D., Badger M.R., Woodger F.J. & Long B.M. (2008) Advances in understanding the cyanobacterial CO_2-concentrating-mechanism (CCM): functional components, C_i transporters, diversity, genetic regulation and prospects for engineering into plants. *Journal of Experimental Botany* **59**, 1441–1461.

Rengstl B., Oster U., Stengel A. & Nickelsen J. (2011) An intermediate membrane subfraction in cyanobacteria is involved in an assembly network for photosystem II biogenesis. *Journal of Biological Chemistry* **286**, 21944–21951.

Rengstl B., Knoppová J., Komenda J. & Nickelsen J. (2013) Characterization of a *Synechocystis* double mutant lacking the photosystem II assembly factors YCF48 and Sll0933. *Planta* **237**, 471–80.

Sacharz J., Bryan S.J., Yu J., Burroughs N.J., Spence E.M., Nixon P.J. & Mullineaux C.W. (2015) Sub-cellular location of FtsH proteases in the

cyanobacterium *Synechocystis* sp. PCC 6803 suggests localised PSII repair zones in the thylakoid membranes. *Molecular Microbiology* **96**, 448–462.
Schottkowski M., Gkalympoudis S., Tzekova N., Stelljes C., Schünemann D., Ankele E. & Nickelsen J. (2009a) Interaction of the periplasmic PratA factor and the PsbA (D1) protein during biogenesis of photosystem II in *Synechocystis* sp. PCC 6803. *Journal of Biological Chemistry* **284**, 1813–1819.
Schottkowski M., Ratke J., Oster U., Nowaczyk M. & Nickelsen J. (2009b) Pitt, a novel tetratricopeptide repeat protein involved in light-dependent chlorophyll biosynthesis and thylakoid membrane biogenesis in *Synechocystis* sp. PCC 6803. *Molecular Plant* **2**, 1289–1297.
Stengel A., Gügel I.L., Hilger D., Rengstl B., Jung H. & Nickelsen J. (2012) Initial steps of photosystem II de novo assembly and preloading with manganese take place in biogenesis centers in *Synechocystis*. *The Plant Cell* **24**, 660–675.
van de Meene A., Hohmann-Marriott M., Vermaas W. & Roberson R. (2006) The three-dimensional structure of the cyanobacterium *Synechocystis* sp. PCC 6803. *Archives of Microbiology* **184**, 259–70.
Vicente J.B., Gomes C.M., Wasserfallen A. & Teixeira M. (2002) Module fusion in an A-type flavoprotein from the cyanobacterium Synechocystis condenses a multiple component pathway in a single polypeptide chain. *Biochemical and Biophysical Research Communications* **294**: 82–87.
Vicente J.B., Carrondo M.A., Teixeira M. & Frazão C. (2008a) Structural studies on flavodiiron proteins. *Methods in Enzymology* **437**, 3–19.
Vicente J.B., Justino M.C., Gonçalves V.L., Saraiva L.M. & Teixeira M. (2008b) Biochemical, spectroscopic, and thermodynamic properties of flavodiiron proteins. *Methods in Enzymology* **437**, 21–45.
Vicente J.B., Testa F., Mastronicola D., Forte E., Sarti P., Teixeira M. & Giuffrè A. (2009) Redox properties of the oxygen-detoxifying flavodiiron protein from the human parasite *Giardia intestinalis*. *Archives of Biochemistry and Biophysics* **488**, 9–13.
Wasserfallen A., Ragettli S., Jouanneau Y. & Leisinger T. (1998) A family of flavoproteins in the domains Archaea and Bacteria. *European Journal of Biochemistry* **254**, 325–332.
Westphal S., Heins L., Soll J. & Vothknecht U.C. (2001) *Vipp1* deletion mutant of *Synechocystis*: a connection between bacterial phage shock and thylakoid biogenesis? *Proceedings of the National Academy of Sciences USA* **98**, 4243–48.
Williams J.G.K. (1988) Construction of specific mutations in photosystem II photosynthetic reaction center by genetic engineering methods in *Synechocystis* 6803. *Methods in Enzymology* **167**, 766–778.
Zhang P., Allahverdiyeva Y., Eisenhut M. & Aro E.M. (2009) Flavodiiron proteins in oxygenic photosynthetic organisms: Photoprotection of photosystem II by Flv2 and Flv4 in *Synechocystis* sp. PCC 6803. *PLoS ONE* **4**, e5331.
Zhang P., Eisenhut M., Brandt A.M., Carmel D., Silén H.M., Vass I., …, Aro EM. (2012) Operon *flv4-flv2* provides cyanobacterial photosystem II with flexibility of electron transfer. *The Plant Cell* **24**, 1952–1971.

Received 8 September 2016; received in revised form 17 November 2016; accepted for publication 20 November 2016

SUPPORTING INFORMATION

Additional Supporting Information may be found in the online version of this article at the publisher's web-site:

Supplemental Figure S1. A schematic map of the plasmid pSll0218-YFP. The *sll0218* ORF and downstream region are indicated in orange. The eYFP-6His gene is indicated in yellow. The ampicillin and spectinomycin resistance cassettes are represented in green.
Supplemental Figure S2. Degradation of D1 protein in WT, Δ*sll0218* and Δ*sll0218-flv2* strains. Protein extracts of cells exposed to 1000 μmol photons m^{-2} s^{-1} for 1,3 and 5 hours in the presence of lincomycin (300 μg mL^{-1}) were equally loaded (20 μg) on SDS-PAGE gels and analyzed by immunoblotting with D1 antibodies. The D1 protein quantification was achieved with a GeneTool (PerkinElmer) software from two biological replicates (maximum SD of ± 20%).
Supplemental Figure S3. A. Observation of two D1-containing intermediates in the Δ*sll0218* strain. Immunoblotting was performed with D1 antibody. **B.** TM complexes from WT, *flv4-2* operon mutants and the Δ*ycf48* mutant were separated by BN-PAGE (100 μg thylakoid extracts per lane) and analyzed by immunoblotting with YCF48 antibody. Red arrows indicate the D1-YCF48-containing intermediate; yellow arrows indicate the RC* complex.
Supplemental Figure S4. Protein extracts (20 μg) from WT and *flv4-2* operon mutants were separated by SDS-PAGE and analyzed by immunoblotting with Phb3 (Slr1128) antibody.
Supplemental Figure S5. Protein extracts (40 μg) of WT, Δ*flv4* and Sll0218-YFP strains were separated by SDS-PAGE and analyzed by immunoblotting with Sll0218 and YFP antibodies. The Sll0218-YFP fusion protein could be detected at the expected mass of about 50 KDa with both the Sll0218 and YFP antibodies.
Supplemental Figure S6. F_0 values of WT and different *flv4-2* operon mutants. The F_0 values were obtained from PAM fluorescence induction curves. Values are means ± SD of four independent experiments.